water

MDPI

Article

Yerba Mate (*Ilex paraguarensis*) as Bio-Adsorbent for the Removal of Methylene Blue, Remazol Brilliant Blue and Chromium Hexavalent: Thermodynamic and Kinetic Studies

Leone Mazzeo [1,2,*], Irene Bavasso [1], Maria Paola Bracciale [1], Marco Cocchi [2], Luca Di Palma [1] and Vincenzo Piemonte [2]

[1] Department of Chemical Engineering Materials & Environment, Sapienza University of Rome, Via Eudossiana, 18, 00184 Rome, Italy; irene.bavasso@uniroma1.it (I.B.); mariapaola.bracciale@uniroma1.it (M.P.B.); luca.dipalma@uniroma1.it (L.D.P.)

[2] Department of Engineering, University Campus Biomedico of Rome, Via Alvaro del Portillo, 21, 00128 Rome, Italy; m.cocchi@unicampus.it (M.C.); v.piemonte@unicampus.it (V.P.)

* Correspondence: leone.mazzeo@uniroma1.it

Received: 15 May 2020; Accepted: 14 July 2020; Published: 16 July 2020

Abstract: Yerba mate (*Ilex paraguarensis*, YM) was used as biomaterial for the removal of anionic and cationic compounds from wastewater. Chromium hexavalent Cr(VI), Remazol brilliant blue (RBB) and methylene blue (MB) were selected as pollutants. A calcination step was performed after the washing and drying steps to evaluate its effectiveness at increasing the adsorption capacity of the solid. Both YM and calcinated YM (CYM) were characterized by means of scanning electron microscopy (FE-SEM), Fourier transform infrared spectroscopy (FT-IR) and Brunauer–Emmett–Teller (BET) analysis. Adsorption batch tests revealed that YM was ineffective for the removal of Cr(VI) and RBB, while good results were obtained for MB (up to 80%) without pH dependency of the adsorption process, and CYM was able to remove Cr(VI) (up to 77%) and RBB (up to 65%) but not MB. The adsorption isotherm of MB on YM at 298 K was obtained experimentally and it is well represented by the Langmuir isotherm. YM's adsorption capacity for MB was estimated to be 59.6 mg/g. Kinetic batch tests were conducted and the experimental results were fitted with a mathematical model. The low influence of temperature compared to the influence of the YM concentration on the adsorption rate was explained.

Keywords: yerba mate; adsorption; hexavalent chromium; methylene blue; Remazol brilliant blue; kinetic study

1. Introduction

Water is an essential element for life and it is mandatory to preserve its quality. With the development of urbanization and industrialization, water pollution has become a major environmental concern.

The release of harmful substances from different anthropogenic sources can in fact compromise water quality [1]. The presence of toxic materials in water strictly depends on the type of activity of origin. For example, the textile and leather sectors are responsible for the release of organic compounds such as pigments and dyes that compromise the quality of water by decreasing the penetration of light or gas dissolution, therefore inhibiting the biological photosynthetic process [2,3]. In industrial wastewaters, dyes are co-present with heavy metals, which is another category of pollutants with dangerous effects on the health of biological species, even at low concentrations, in the aquatic system [4]. Excessive concentrations of, or long-term exposure to, heavy metals cause several health

issues, such as nervous system disorders and irreversible multi-organ failure [5]. Chromium is one of the most toxic heavy metals, and it is released into water bodies as a consequence of industrial activities, such as those of tanneries and metal finishing plants [6]. It exists in two forms, Cr(III) and Cr(VI): the first, Cr(III), is less soluble in the water body, and trace concentrations of Cr(III) are important in carbohydrate metabolism [7]; the second, Cr(VI), is a non-essential element which is toxic and very mobile, with its high oxidizing capacity being correlated with carcinogenic and mutagenic diseases [7,8]. In tannery wastewater, the Cr(VI) concentration can be up to 50 mg/L [7], while 0.1 mg/L is the admitted level of Cr(VI) in surface water [9].

Several technologies have been proposed for the removal of these pollutants: dyes have been removed through chemo-physical [10] or electrochemical [11] methods or, nowadays, by the synergic effect of UV, ozone and H_2O_2 as an advanced oxidation process [12]. Heavy metal removal has been performed by traditional methods (chemical precipitation, filtration, ion exchange, electrolysis, coagulation, electrocoagulation) that were intensively adopted but are limited by the high cost [13]. In the case of innovative methods, the use of reactive nanoparticles such as nano-zerovalent iron is a valid solution for the removal of heavy metals, especially Cr(VI), because they enable its reduction into the (III) valent oxidation form [14].

Adsorption is a traditional and low-cost method (compared to other traditional processes), with a high removal efficiency of dye and heavy metals [15,16], especially with the adoption of activated carbon [17,18]. To lower the cost and the environmental impact of these materials [8], a lignocellulosic precursor for activated carbon production has been intensively studied [19,20]. Other low-cost alternatives are natural materials (clay minerals, zeolites and siliceous materials) [21,22] or "residual biomasses" such as agro-based by-products like vine shoots [23], grape stalks [24], cherry kernels [25] and Camellia oleifera seed shells [8]. These biomasses are attracting increased attention because the materials can be found easily as waste or by-products at almost no cost [26].

Yerba mate (*Ilex paraguariensis*) is a tea-like plant produced in South American countries; nowadays, 280,000 tons per year are domestically produced in Argentina [27], and an increase in its consumption will be expected over the next few years [28]. The tea, called "mate", is prepared by the infusion of mate leaves; this extract is rich in polyphenols, xanthines, alkaloids, flavonoids, vitamins and minerals [29,30]. The potential benefits of this material can also be found in its waste. The extract can be used as a reducing agent for the green synthesis of nanoparticles [28] or the re-use of solid residue for the production of materials for thermal insulation purposes [31]. The solid is a prominent material for adsorption processes: activated carbon can be produced from yerba mate (YM) due to the presence of oxygenated acid groups, which makes it ideal for phenol adsorption [32]; the presence of several functional groups suggests its possible application for the adsorption of dyes without pre-treatment [33].

In the present study, the use of large-sized particles from YM solid waste in the adsorption of Cr(VI) and dye pigments was investigated. Methylene blue (MB) and Remazol brilliant blue (RBB) were tested as cationic and anionic dyes, respectively. Adsorption tests were performed at different pH conditions (from 3 to 10), different temperatures (from 283 K to 313 K) and different dosages of YM and pollutant concentrations. Scanning electron microscopy (FE-SEM), Fourier transform infrared spectroscopy (FT-IR) and Brunauer–Emmett–Teller (BET) analysis were conducted in order to offer a complete characterization of the adopted material. Good results in terms of MB removal (up to 80%) were achieved, while low Cr(VI) removal and limited RBB adsorption rates were observed. This critical aspect was overcome by proposing a calcination step for the pre-treatment of the adsorbent material.

2. Materials and Methods

2.1. Material Preparation and Characterization

2.1.1. Bio-Adsorbent Preparation

The yerba mate (YM) waste was obtained as a residue of beverage production. The waste was washed 5 times in boiled demineralized water, dried in an oven at 333 K and chopped with a

twin-function mill. A standard stainless-steel sieve system was used for the solid particle separation, and the particles with diameters in the range of 1.19–2.00 mm were tested as bio-adsorbents.

Additional tests were carried out using calcinated yerba mate (CYM) [34] to evaluate the possible activation effect of waste on the adsorption of anionic species. The calcinated material was produced by treating the selected solid fraction in a muffle furnace at 600 °C for 1 h.

2.1.2. Chemicals

Methylene blue ($C_{16}H_{18}ClN_3S$; MB), Remazol brilliant blue ($C_{22}H_{16}N_2Na_2O_{11}S_3$; RBB), potassium dichromate ($K_2Cr_2O_7$), 1,5-diphenylcarbazide ($C_{13}H_{14}N_4O$), hydrochloric acid (HCl) and sodium hydroxide (NaOH) were purchased from Sigma Aldrich (United States). All chemicals were of analytical reagent grade and used without any further purification. The solutions used in the experimental tests were prepared by providing a dilution in ultra-pure water.

2.1.3. Analysis

A morphological investigation of YM and CYM was performed using a field-emission scanning electron microscope (HR-FESEM AURIGA, Zeiss, Germany). The samples were prior sputter-coated with a 10 nm thin layer of chromium using a Quorumteach Q150T sputter coater.

The functional groups on the surfaces of the samples were detected by Fourier transform infrared (FT-IR) spectroscopy. Infrared measurements were carried out with a Bruker Vertex 70 spectrometer (Bruker Optik GmbH, Germany) equipped with a single reflection Diamond ATR cell. Spectra were recorded with a 3 cm^{-1} spectral resolution in the mid infrared range (400–4000 cm^{-1}), using 512 scans. Yerba mate samples were ground, quartered and run in triplicate.

The specific surface area (SSA) was measured by N_2 adsorption–desorption isotherms acquired at 77 K using a Micromeritics 3Flex analyzer (Micromeritics Instrument Corp., USA). The adsorption–desorption isotherms were acquired in the p/p^0 range of 0.01 to 0.99. Samples were previously outgassed at 423 K for 3 h. The BET (Brunauer–Emmett–Teller) and BJH (Barrett–Joyner–Halenda) equations were used to determine the specific surface area, pore volume and average pore diameter, respectively [35].

The zero charge point (pH_{PZC}) was determined according to the pH drift method [36]. A volume of 0.5 g of YM was added to 50 mL of ultra-pure water. Before the addition of the solid, the pH of the solution was adjusted from 2 to 12 by the addition of HCl (0.1 M) and NaOH (0.1 M). The suspension was placed on an orbital shaker for 24 h to reach the equilibrium condition. After this, the final pH was measured, and the pH_{PZC} was determined as the point at which the final pH is equal to the initial pH of the solution. The pH measurement was performed using a Crison GLP 421 pH meter (Hach Company, Crison, Spain).

The adsorption of dyes was measured by spectrophotometric analysis using a PG Instruments (United States) T80+ UV/Vis spectrophotometer (with glass cells of 1 cm path length) at λ = 674 nm (MB) and λ = 591 nm (RBB). The spectrophotometer analysis was also adopted for the Cr(VI) adsorption tests by the colorimetric method, using 1,5-diphenylcarbazide [37].

2.1.4. YM Characterization

The infrared spectra of the samples of neat YM waste shown in Figure 1 exhibit the characteristic bands of a lignocellulosic material. A detailed assignment of the main bands in yerba mate waste spectra is reported elsewhere [38]. Upon calcination, the complete removal of main bands related to hemicellulose (1732, 1238 and 591 cm^{-1}), cellulose (1422, 1318, 1107, 664 and 559 cm^{-1}), xanthines (1644 cm^{-1}) and lignin (1594, 1504 and 1455 cm^{-1}) components, initially present in the YM residue, was conducted.

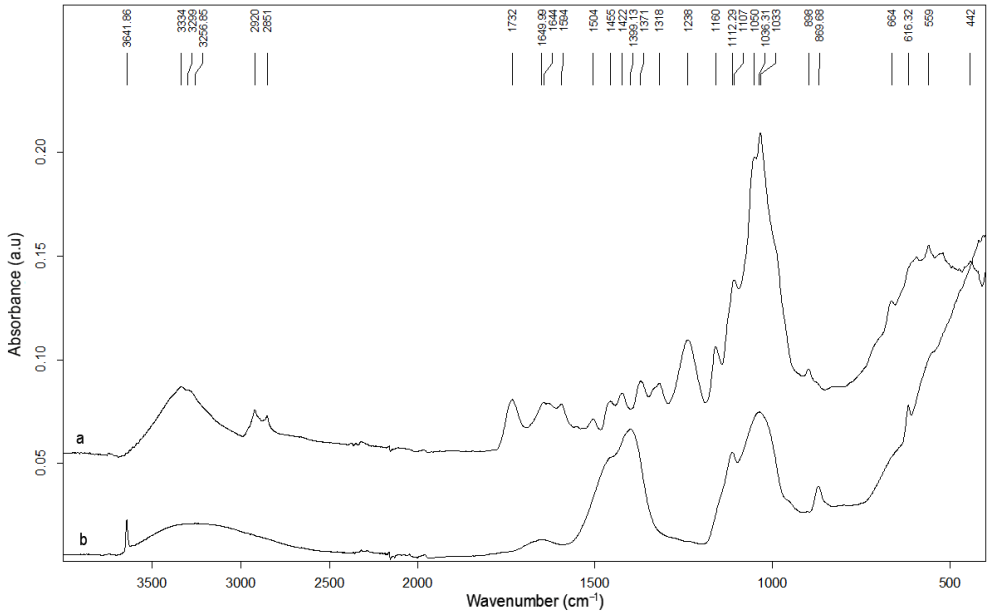

Figure 1. Infrared spectra of the yerba mate (YM) (**a**) and calcinated yerba mate (CYM) (**b**) samples.

The extremely sharp band at 3642 cm^{-1} in CYM could be ascribed to OH stretching, which may arise due to the retaining of some hydroxides, such as $Ca(OH)_2$, $Mg(OH)_2$, Si-OH, etc. The absorption bands at 1457 and 870 cm^{-1} are assigned to different vibration modes C-O of carbonate groups $CO_3^{=}$. The other bands at 1399, 1112 and 1050 cm^{-1} are attributed to C-H, C-O-H (OH deformations of carboxyl-C) and C-O (alkyl/aryl ethers), respectively [39].

In the FE-SEM micrographs of YM shown in Figure 2a,b, a coarse surface topography with a large number of pores can be observed. This morphology could provide the dye with a greater dye adsorption capacity by such bio-adsorbents due to the capture of contaminants in its irregular internal surface area. The internal structure of the calcinated YM (CYM) was different, and a fibrous aspect (Figure 2c) with a large prismatic hexagonal crystal of calcium hydroxide (Figure 2d) can be clearly detected.

The BET specific surface area (BET SSA) showed an important increase by 1.08 ± 0.02 m^2/g to 13.84 ± 0.06 m^2/g when the YM samples were thermally treated (Table 1). This result supports the employment of this material as an adsorbent in the treatment of refractory organic pollutants such as dyes. Similar values of YM specific surface area were found in [33].

Table 1. Specific surface area (SSA) of YM samples.

Sample	Surface Area (m^2/g)	Pore Volume (cm^3/g) (×10^{-3})	Average Pore Diameter (Å)
YM	1.08	0.48	17.85
CYM	13.84	59	183.39

From the data displayed in Figure 3, pH_{PZC} of YM was estimated to be equal to 6.52. At pH conditions lower than pH_{PZC}, the presence of a positive charge on the YM surface could promote the adsorption of anionic species, whilst, due to the absence of any protonation, for pH conditions higher than pH_{PZC}, the adsorption of cationic species will be promoted [40].

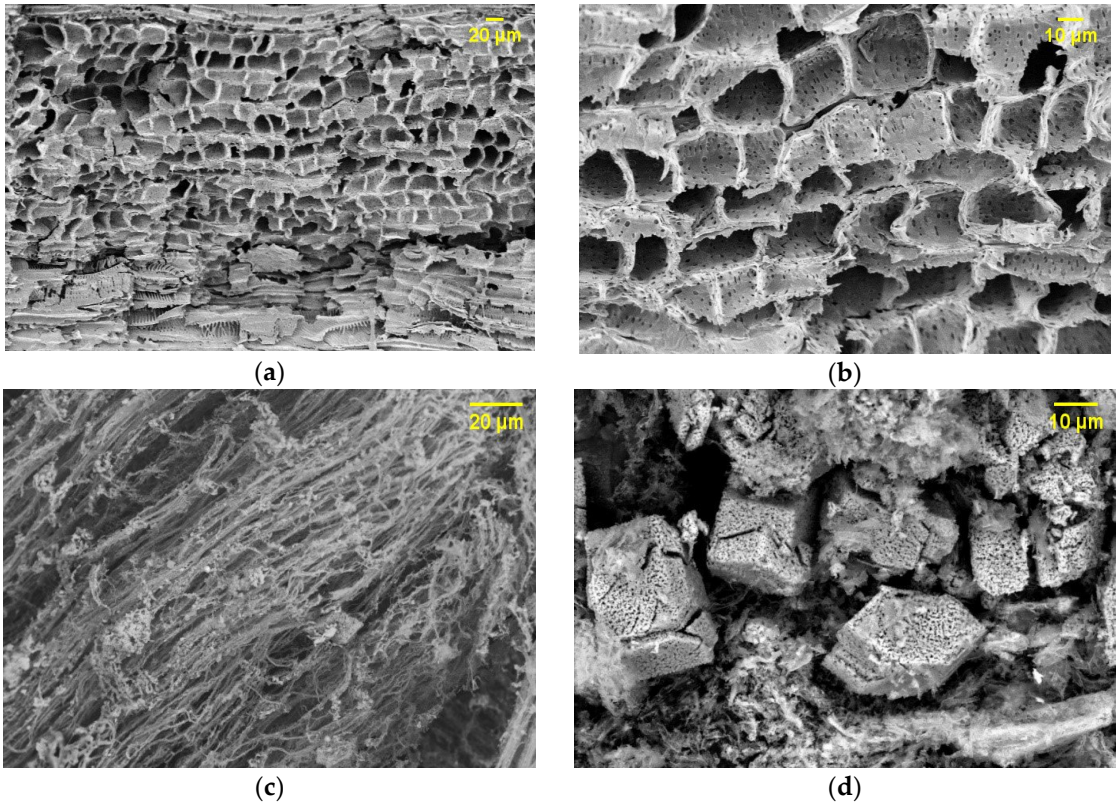

Figure 2. FE-SEM micrographs of the YM (**a**,**b**) and CYM (**c**,**d**) samples.

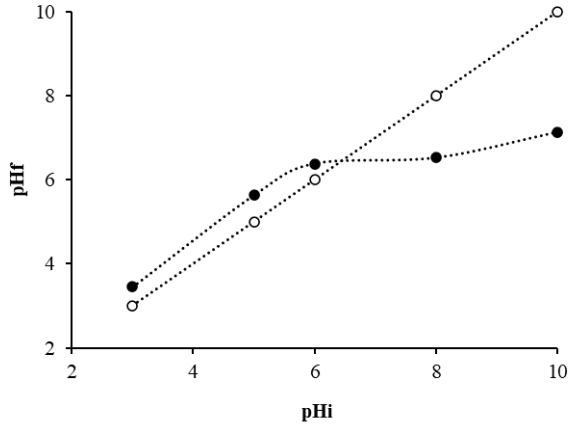

Figure 3. Zero charge point (pHpzc) of YM, determined by the pH drift method. The zero charge point is represented by the intersection of the two curves: the black dotted (•) curve shows the final pH (pHf) of the suspension with respect to the initial one (pHi); the white dotted curve (o) represents the condition pHi = pHf.

2.2. *Adsorption Tests*

Preliminary tests as investigations of the adsorption efficiency of both dyes and Cr(VI) were performed at different pH conditions by mixing 0.2 g of bio-adsorbent (YM or CYM) in 50 mL, with a pollutant concentration of 20 mg/L. The solutions were stirred in an orbital shaker until equilibrium (72 h) at 298 K. The percentage of the pollutant i that was removed (Ei) was calculated with the following equation:

$$E_i\ (\%) = ((C_{i0} - C_{i,e})/C_{i0}) \times 100 \quad (1)$$

where C_{i0} is the concentration (mg/L) of the pollutant at the beginning of the test and $C_{i,e}$ is the concentration of the pollutant at equilibrium (mg/L). Using YM, surprisingly, no adsorption effect of RBB and Cr(VI) was observed, while a removal of MB of 81.85 %, 71.58 %, 74.36 % and 72.90 % at pH = 10, pH = 8, pH = 6 and pH = 4 was calculated, respectively. These results are quite different from those observed by Aldbadarin and co-workers, where the removal of an anionic dye (orange II sodium salt) and MB was successfully achieved in different pH conditions (2.04 and 8.98, respectively) thanks to the presence of different functional groups in the fraction of YM used [33]. A discussion of the adsorption process of the anionic species will be reported later. Although there is no significant effect of pH, the dosage of adsorbent material plays a key role in the adsorption process. In an attempt to define the best operative conditions of the MB adsorption process, tests at different YM dosages were performed at 298 K with 50 mL of MB solution (20 mg/L). After 72 h, the MB residue concentration was measured, and the results are reported in Figure 4. An initial growing trend was observed with the increase of YM dosage up to 1.6 g/L, where a slowdown in the process was observed. Beyond this value, a further increase in the dosage of solid did not contribute significantly to MB removal, which reached a value of 80%. At low dosages of YM, the availability of active sites for the adsorption was a limiting factor, while at dosages higher than 1.6 g/L, the efficiency of the process was controlled by the mass transfer of MB diffusion onto YM [41].

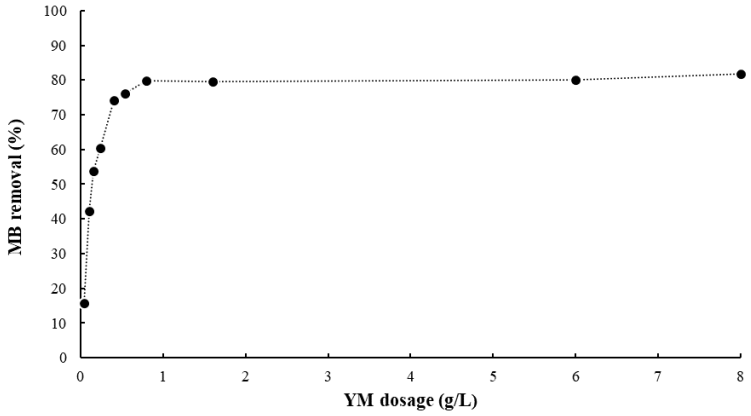

Figure 4. Methylene blue (MB) adsorption removal efficiency after 72 h of equilibrium tests at different YM dosages. Conditions: 20 mg/L of MB, 50 mL of volume, pH = 6 and 25 °C.

The reusability of the YM was investigated by performing a desorption cycle in 0.1 M of HCl solution, in accordance with other authors [7]. After 24 h of the desorption cycle, the solid was washed several times, then dried and re-used in the adsorption test, with 0.5 g of YM in 50 mL of MB solution (20 mg/L) at room temperature (298 K) and pH = 6. In such conditions, removal rates of 58% and 41% were reached after the first and second pre-treatment cycles, respectively, compared to a removal of 64% obtained with the first use of YM. This result highlighted the fact that after the second regeneration cycle, a significative decrease in the MB removal of about 36% was calculated, demonstrating that further evaluations of the type of pre-treatment and removal efficiency are required if more than three reuses of the material are necessary.

2.3. MB Adsorption Batch Tests Using YM

2.3.1. Isotherm and Thermodynamic Studies

A solution of 50 mL of MB with 4 g/L of YM was placed in a 100 mL conical flask and shaken for 72 h. The concentrations of MB ranged from 20 to 350 mg/L and the temperature was fixed at 298 K. The suspension was centrifuged, and the supernatant was analyzed for the detection of MB concentration. To determine the equilibrium adsorption capacity of YM, the equilibrium concentrations

of MB were compared to the Langmuir (Equation (2)) and Freundlich (Equation (3)) isotherm models, expressed by the equations below:

$$q_e = (q_{max}\ b\ C_{MB,e})/(1 + b\ C_{MB,e}) \quad (2)$$

$$qe = k_F\ C_{MB,e}\hat{}(1/n_F) \quad (3)$$

where b (L/mg) is the equilibrium constant of the Langmuir model correlated to the affinity of binding sites, q_{max} (mg/g) is the maximum adsorption capacity, q_e (mg/g) is the equilibrium adsorption capacity and $C_{MB,e}$ (mg/L) is the equilibrium concentration of MB in the liquid phase. The Freundlich isotherm is an empirical equation used to describe heterogeneous surfaces with a distribution of heats of adsorption, where k_F ((mg/g) (L/mg)$^{(1/nF)}$) is the distribution coefficient and $1/n_F$ is a correction factor. The constants of both isotherms were obtained by a non-linear fitting of the experimental data based on the minimization of the mean square error.

The standard free energy change, ΔG° (kJ/mol), at 298 K was then calculated with the following relation:

$$\Delta G^\circ = -\mathbf{R}\ T\ \ln(b\ PM \times 10^3) \quad (4)$$

where **R** (8.314 J/mol K) is the universal gas constant, T (K) is the absolute temperature and PM (g/mol) is the molecular weight of the adsorbed compound.

2.3.2. Kinetic Studies

The kinetic batch tests were performed in a 100 mL conical flask with 50 mL of MB solution at pH 6 shaken for 4 h (time enough to reach the equilibrium) in an oscillator system. During the tests, the suspension was centrifuged, and the supernatant was analyzed for the detection of MB concentration. Adsorption tests were performed at different bio-adsorbent dosages and pollutant concentrations in a fixed ratio, R, as outlined by Equation (5):

$$R = x_s/C_{MB0} \quad (5)$$

where x_s is the bio-adsorbent concentration (mg/L) and C_{MB0} is the concentration (mg/L) of MB at the beginning of the test. The adsorption process was studied at different R values by varying the operative temperature (283 K, 293 K and 313 K). More precisely, for each temperature, the parameter R was varied, changing the bio-adsorbent dosage while keeping the starting concentration of MB constant. Table 2 reports all the concentrations of bio-adsorbent adopted for each temperature.

Table 2. Bio-adsorbent concentrations in batch tests.

R (mg/mg)	x_s (mg/L) × 10^{-3}		
	283 K	**293 K**	**313 K**
100	2.6	2.4	2.5
200	5.3	4.8	5.1
300	7.9	7.3	7.7

A mathematical model was developed in order to analyze and predict the adsorption kinetics mechanism in different adopted conditions. The modeling is based on the linear driving force (LDF) model assumptions [42] and some other hypotheses:

- Perfect mixing conditions of the solid/liquid mixture;
- Homogeneous concentration of MB adsorbed through the solid particle:

$$q = q_e \quad (6)$$

where q is the volume-averaged amount of MB adsorbed per mass of adsorbent (mg/g).

- The mass rate of MB from the liquid to the solid phase is described by Equation (7), written below:

$$F = k_C \, \alpha \, x_s \, (C_{MB} - C^*_{MB,e}) \, V \quad (7)$$

where F is the mass transfer rate (mg/min), k_C is the LDF mass transfer coefficient (dm/min), α is the specific surface area of the adsorbent (YM), set equal to 0.108 dm^2/mg, as reported in Table 1, x_s is the bio-adsorbent concentration (mg/L), C_{MB} is the concentration of MB in the liquid bulk (mg/L), $C^*_{MB,e}$ is the MB concentration of a hypothetic liquid phase in equilibrium with the "bulk" of the solid phase (mg/L) and V is the liquid volume (L).

- The system at equilibrium is well represented by the Langmuir isotherm.
- The product of the Langmuir constant (b) and the concentration at equilibrium of MB in the hypothetic liquid solution ($C^*_{MB,e}$) satisfies the condition $b \, C^*_{MB,e} \ll 1$, leading to the simplification being verified when the discussing the results.

$$q_e = (q_{max} \, b \, C^*_{MB,e})/(1 + b \, C^*_{MB,e}) \approx q_{max} \, b \, C^*_{MB,e} \quad (8)$$

A system of two differential equations was set:

$$dC_{MB}/dt = -k_L \, \alpha \, x_s \, (C_{MB} - C^*_{MB,e}) \quad (9)$$

$$dq/dt = k_L \, \alpha \, x_s \, (C_{MB} - C^*_{MB,e}) \quad (10)$$

remembering that $C^*_{MB,e}$ is linked to q by Equation (6) and Equation (8). The initial conditions of the system were as follows:

$$C_{MB}(0) = C_{MB0} \quad (11)$$

$$q(0) = 0 \quad (12)$$

The system admitted an analytical solution, which was as follows:

$$C_{MB}(t)/C_{MB0} = 1 - [x_s/(x_s + 1/(q_{max} \, b))] \, \{1 - \exp(-(x_s + 1/(q_{max} \, b))(k_C \, \alpha)t)\} \quad (13)$$

A non-linear regression, based on the minimization of the mean square error, was performed for the determination of the parameters q_{max} b and k_C for each test.

Additional tests at R = 200 and R = 400, both at 298 K, with solid concentrations of 3.54 and 7.08 g/L, respectively, were carried out in order to validate the model.

3. Results and Discussion

3.1. Isotherm and Thermodynamic Studies

In order to compare yerba mate with other types of bio-adsorbents, isotherm data at 298 K were collected: Langmuir and Freundlich constants, derived from fitting, were used to quantify the maximum adsorption capacity of YM. The reported experimental results are mean values of at least three repetitions and are plotted in Figure 5, together with the Langmuir and Freundlich isotherms. The mean square error obtained from isotherm fitting was 9.3 for Langmuir and 15.6 for Freundlich. According to such considerations and since the experimental data in Figure 5 show a saturation behavior typical of the Langmuir isotherm, it is clear that the Langmuir isotherm provides a better representation of the system.

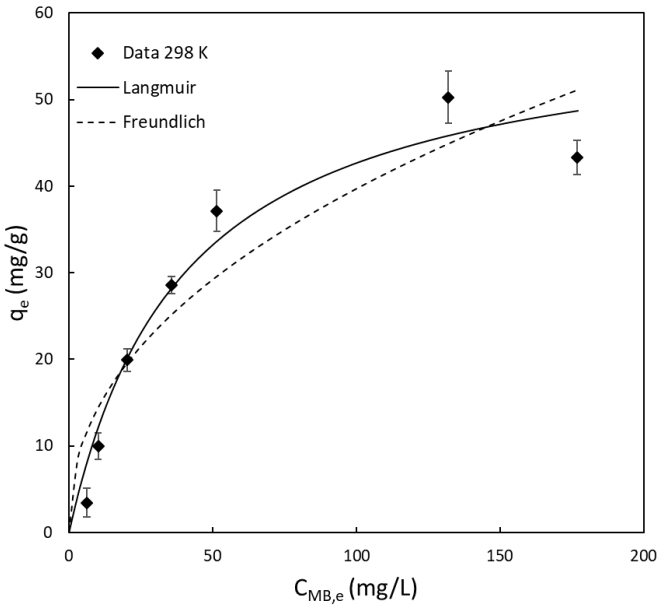

Figure 5. Langmuir and Freundlich isotherms obtained by a non-linear fitting of the adsorption data of MB using yerba mate at 298 K. The error bars represent the standard deviation.

The Langmuir and Freundlich constants obtained are reported in Table 3, where they are compared with the same parameters calculated for other bio-adsorbent materials reported elsewhere. The comparison shows that YM has a higher adsorption capacity (q_{max}) than most of the other bio-adsorbents, such as chaff [43], peanut hull [44], banana peel [45], orange peel [45], rice husk [46], apricot shells [47], wheat shells [48], spent coffee grounds [49] and passion fruit waste [50]. Only the study conducted by Uddin et al. on tea wastes [51] reveals a higher adsorption capacity than yerba mate, which was also promoted by the high specific surface area of the particles adopted in the adsorption tests (180–300 μm) compared to the material tested in the present study. To the best of our knowledge, no other studies regarding bio-adsorbents derived from the food industry have been extensively studied in the literature, establishing yerba mate as one of the most promising solid adsorbents in this field.

Table 3. Comparison of the Langmuir and Freundlich constants for different types of food waste bio-adsorbents.

Bio-Adsorbent	T (K)	pH	Langmuir		Freundlich	
			q_{max} (mg/g)	b (L/mg)	K_F	n
Yerba mate (This study)	298	6	59.6	0.02	5.17	2.26
Tea waste [51]	298	8	85.16	1.26	46.81	1.51
Chaff [43]	298	7	20.03	0.22	4.92	2.83
Peanut hull [44]	293	5	60.05	0.16	9.11	1.89
Banana peel [45]	303	7	20.8	0.06	1.34	3.03
Orange peel [45]	303	7	18.6	0.05	1.75	3.85
Rice husk [46]	305	8	40.5	0.14	8.62	2.75
Apricot shells [47]	298	5	24.31	0.002	14.66	3.44
Wheat shells [48]	303	7	16.56	0.02	1.46	2.74
Spent coffee grounds [49]	298	5	18.72	0.27	5.19	3.30
Passion fruit waste [50]	298	8	44.70	0.002	0.40	1.49

The variation in the standard free energy calculated by Equation (4) is $\Delta G^\circ = -22.3$ kJ/mol, confirming the spontaneity of the process.

3.2. Kinetics Experiments and Fitting of Model Parameters

Kinetics batch tests were carried out to assess the influence of temperature and adsorbent concentration on the adsorption rate. The experimental results are given in terms of the ratio between the adsorbate concentration measured along time and the initial concentration: this allows a better comparison of the graphs. In Figure 6, the experimental points are presented, together with the curve of the model outcome from fitting. The values of the constants q_{max} b and k_C derived from fitting are resumed in Figure 7. As it is possible to see from Figure 6, the increase of the bio-adsorbent concentration from R = 100 to R = 300 enhanced the velocity of the adsorption process, and an increase in MB removal was observed. To evaluate the influence of temperature on the adsorption behavior, more information is given in Figure 7: the values of both parameters q_{max} b and k_C, derived from fitting, were constant for the entire range of temperatures (283 K–313 K), indicating that, in such a range, the temperature had no significant influence on the kinetics of the process. This result can be explained with the following considerations:

- the variation in temperature did not change the liquid properties or the effective diffusivity of MB through YM's pores, and k_C, the overall LDF transport coefficient, remained constant;
- the concentration of MB in the liquid phase at equilibrium was negligible and the variation in the isotherm slope was not appreciable (q_{max} b remains constant).

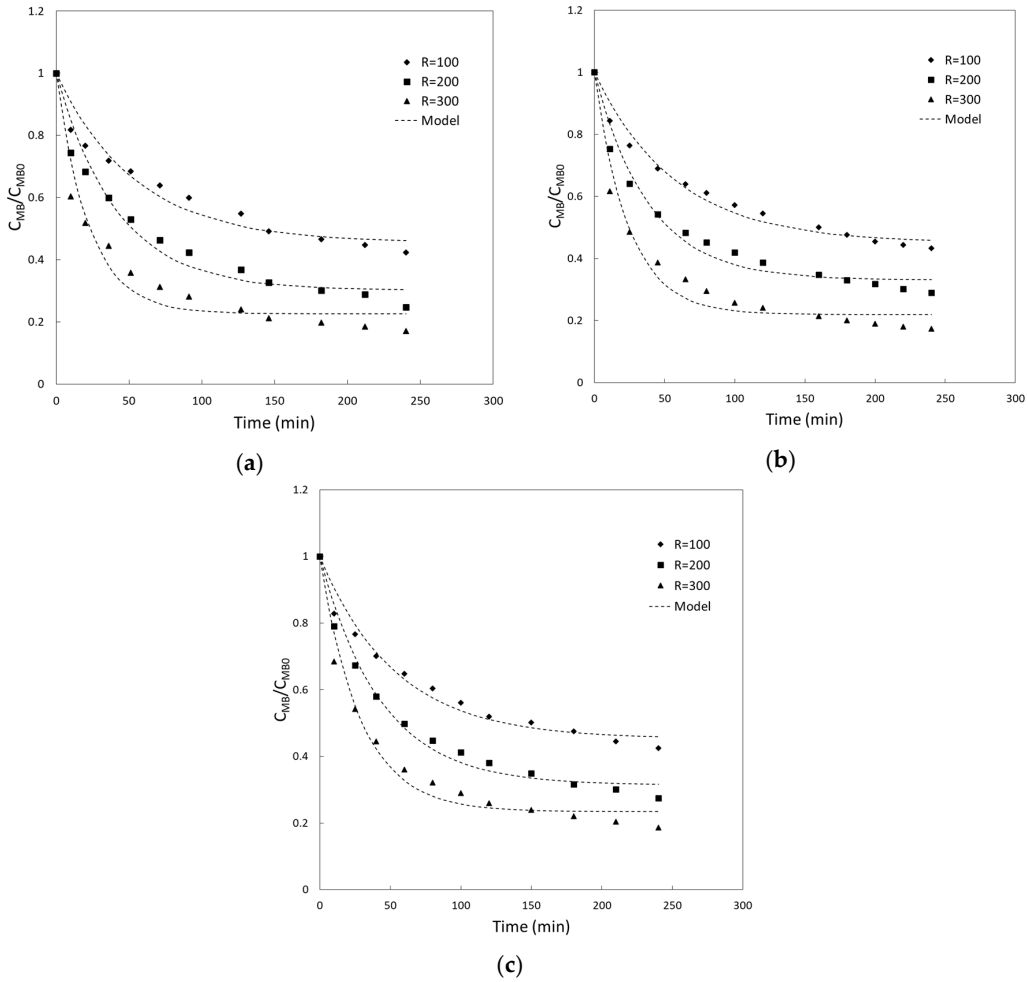

Figure 6. MB adsorption in yerba mate at different R values (100, 200, 300 for each graph) and at temperatures of 283 K (**a**), 293 K (**b**) and 313 K (**c**).

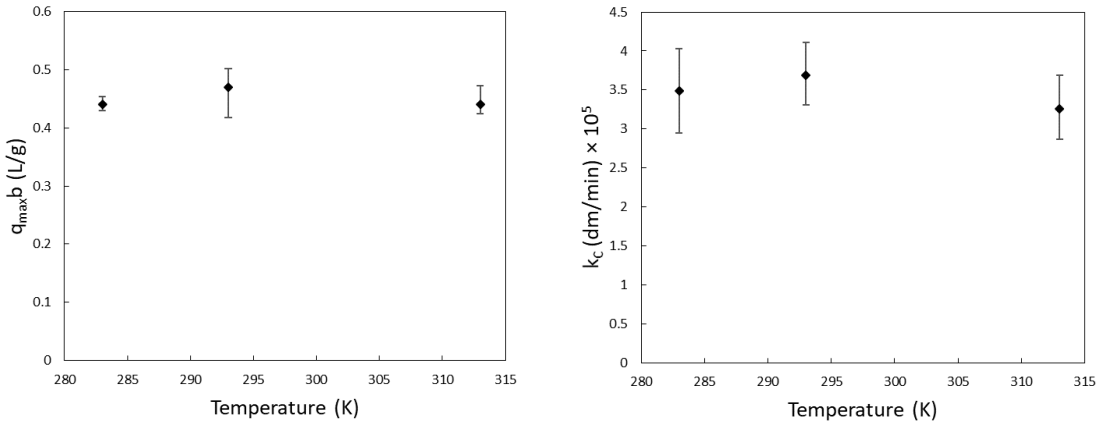

(**a**) (**b**)

Figure 7. Variation of the parameters of fitting q_{max} b (**a**) and k_C (**b**) with temperature. The points reported are the means of the fitting values. Moreover, the error bars represent the maximum and minimum difference between the values of fitting and the mean.

In addition, the equation below describes how k_C depends on the effective diffusivity in the event that the limiting step of the process is the inter-particle pore diffusion [52]:

$$k_C \cong 5\ D_i/R_p \tag{14}$$

where D_i (m^2/s) is the effective diffusivity of the component I, and R_p (m) is the radius of a particle of the adsorbent material. By means of Equation (14), D_{MB} was calculated using $k_C = 3.5 \times 10^{-5}$ (dm/min), which is the mean of all the values of k_C obtained from the fitting (see Figure 7), and R_p = 1 mm (average size of solid particles). It resulted in $D_{MB} = 0.16 \times 10^{-10}$ m^2/s, which is more than one order of magnitude less than the diffusivity of MB in water [53]. Such a significant decrease could be attributed to the resistance of pore diffusion of MB into the bio-adsorbent.

3.2.1. Model Validation

Based on the results previously reported, it is evident that the Langmuir isotherm best represents the equilibrium of the system. At the same time, temperature proved not to be a crucial parameter in the adsorption kinetic of MB on yerba mate in the operative conditions adopted in this work. To confirm the hypothesis expressed by Equation (8), the condition b $C^*_{MB,e} \ll 1$ must be satisfied for the entire duration of the test: when t→0, since almost no material has been adsorbed yet, q→0, which means that $C^*_{MB,e}$→0, and it follows that b $C^*_{MB,e}$→0. When t→∞ and the system approaches equilibrium ($C_{MB} = C^*_{MB,e}$), since the starting concentration of MB in the liquid phase for every test was C_{MB0} < 26 mg/L and the ratio C_{MB}/C_{MB0} was at the maximum of 0.5 (see Figure 6), the result is that it is always $C^*_{MB,e}$ < 13 mg/L and b $C^*_{MB,e}$ < 0.26 (b = 0.02 L/mg calculated from isotherm fitting). As it is possible to see from Figure 5, for an equilibrium concentration of 13 mg/L, the isotherm is still in the linear region, which means that b $C^*_{MB,e}$ < 0.26 is small enough to satisfy the hypothesis of Equation (8).

In order to validate the model proposed in Equation (13), two additional tests were run at 298 K. Such experimental results are compared in Figure 8 against the numerical results (dotted line) of Equation (13), now implemented for the prediction of the adsorption kinetics. The values of the fitting parameter for this simulation were as follows:

- q_{max} b = 0.44 (L/g), taken as the mean of all the values of q_{max} b obtained from the fitting (see Figure 7);
- $k_C = 3.5 \times 10^{-5}$ (dm/min), taken as the mean of all the values of k_C obtained from the fitting (see Figure 7).

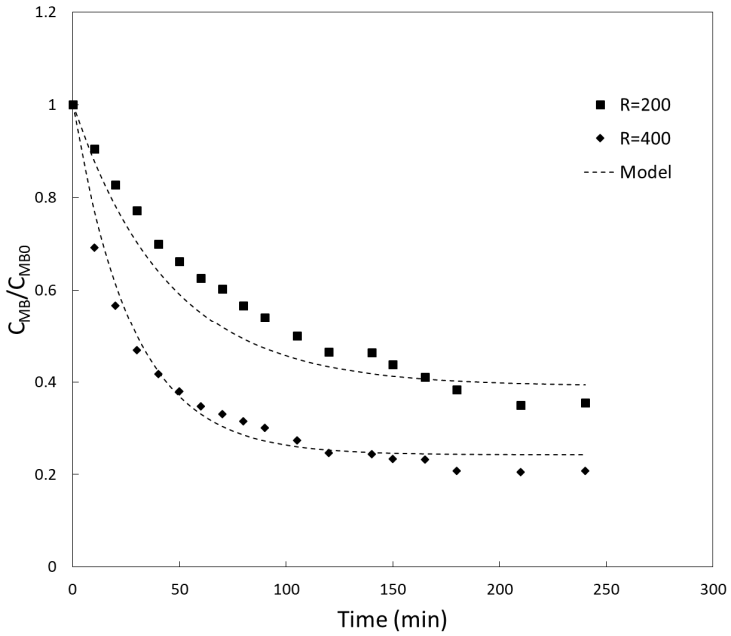

Figure 8. Adsorption kinetics of methylene blue on yerba mate at 298 K for R = 200 and R = 400. The dashed lines represent how the model (with q_{max} b = 0.44 (L/g) and $k_C = 3.5 \times 10^{-5}$ (dm/min)) predicts the trend of adsorption.

As depicted in Figure 8, the model successfully predicted the experimental data, with a mean square error of 0.22 for the case of R = 200 and 0.13 for the case of R = 400.

3.2.2. Characteristic Time of Adsorption

To quantify how the rate of adsorption was influenced by the amount of bio-adsorbent in terms of the parameter R, a characteristic time of adsorption was derived according to the Equation (13):

$$\tau = 1/((x_s + 1/(q_{max}\ b))(k_C\ \alpha) \quad (15)$$

The characteristic time τ (min), as clearly noticeable in Equation (15), depends on the concentration of the bio-adsorbent, specified by x_s (mg/L), and the temperature (intrinsically contained in q_{max} b and k_C α). By means of Equation (15), derived from the model expression, the characteristic time τ (min) was calculated for the tests at 283 K, 293 K and 313 K, using for each test the values of q_{max} b and k_C α derived from fitting. Since it has been previously observed that temperature did not significantly influence the values of the constants q_{max} b and k_C α, the variation in τ was reported only in the function of R in Figure 9. As expected, the characteristic time of adsorption decreased when the concentration of the solid adsorbent increased. More precisely, by doubling the amount of solid adsorbent (from R = 100 to R = 200), the characteristic time of adsorption was reduced by 15 min; by tripling the amount of solid adsorbent (from R = 100 to R = 300), the characteristic time of adsorption was reduced by 30 min.

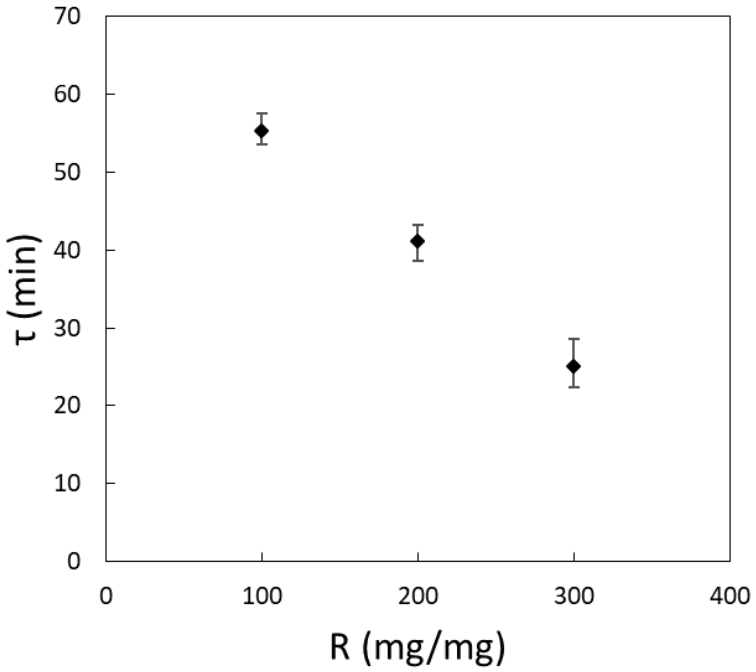

Figure 9. Variation in the characteristic time of adsorption of methylene blue using yerba mate versus R. The points reported are the means of the fitting values. Moreover, the error bars represent the maximum and minimum difference between the values of fitting and the mean.

3.3. Adsorption of RBB and Cr(VI) Using YM and CYM

According to the pH_{ZC} of YM (Figure 3), adsorption tests of the RBB were conducted at maximum pH values of 6 due to the anionic nature of the dye. Unlike the previous results on MB, no satisfying RBB removal was obtained under any experimental condition. The maximum value of RBB removal (27%) was observed at a low pH condition (pH = 3) and low temperature (283 K). This suggested the inapplicability of YM material for the removal of anionic species due to the low availability of protonated species on the coarse fraction of YM waste (as nitrogen based groups [54]) and the presence of functional groups [33] that limit the occurrence of a low distribution of the positive charge (Figure 3). On the contrary, this low presence of positive charge allows the promotion of the adsorption of the cationic species in the investigated pH conditions.

Similar results were obtained during the adsorption tests of Cr(VI). Under acidic pH conditions (up to 3), Cr(VI) existed in the form of $HCrO^{-}{}_4$ and $Cr^2O_7{}^{2-}$ [8], while above pH 7, Cr(VI) exists only in the form of $CrO_4{}^{2-}$ ions, according to the reaction below [55]:

$$Cr^2O_7{}^{2-} + H_2O \leftrightarrow 2\ CrO_4{}^{2-} + 2H^+ \quad (16)$$

Acidic pH conditions are required in order to promote the electrostatic attraction between the negative charge of Cr ions and the surface of YM. However, in this case, due to the low attitude to protonation, a lower Cr(VI) adsorption was observed compared to MB: a 50% removal of Cr(VI) was calculated at 283K and pH = 3. These results represent the best results obtained in the experimental campaign. In the attempt to improve the removal of the anionic species, an activation effect of YM was stimulated by calcinating the waste material. The results of the adsorption test performed at 298K and pH = 6 with YM in the calcinated and non-calcinated form are reported in Table 4.

Table 4. Removal efficiency of MB, Remazol brilliant blue (RBB) and chromium hexavalent Cr(VI) on YM and CYM samples.

Sample	T (K)	pH	E_{RBB} %	$E_{Cr(VI)}$ %	E_{MB} %
YM	283	3	27.00	50.00	70.00
YM	298	6	0	2.80	74.36
CYM	298	6	77.00	65.00	0

Table 4 shows that the activation of YM produced a positive effect on RBB and Cr(VI) adsorption; at a neutral pH condition and 298 K, the removal of MBB and Cr(VI) reached 77% and 65%, respectively, suggesting that it is not necessary to operate in extreme operating conditions (283 K and pH = 3) to ensure effective removal of the species. On the contrary, the removal of MB was completely reset, suggesting that the calcination resulted in the removal of the functional groups responsible for the removal of cationic species.

4. Conclusions

In this work, yerba mate (*Ilex paraguariensis*), an agro-food waste, was tested as a bio-adsorbent for the removal of methylene blue (MB), Remazol brilliant blue (RBB) and Cr(VI) from an aqueous solution. It was observed that YM is an excellent bio-adsorbent for the removal of MB, while it was less effective for the adsorption of RBB and Cr(VI). For this reason, MB adsorption was investigated in more detail, leading to the following conclusions:

- Adsorption of MB using YM is a spontaneous process. The adsorption isotherm follows the Langmuir expression, and an adsorption capacity of 59.6 mg/g was calculated. Compared to other food-derived bio-adsorbents tested in the literature, YM shows one of the highest adsorption capacities;
- The concentration of YM is the most important operative parameter of the bio-adsorption process: an increase in bio-adsorbent concentration speeds up the adsorption process and reduces the residual amount of pollutant in the aqueous solution. The effect of temperature and pH are negligible in the range of concentrations of MB considered.

The additional calcination of the yerba mate waste resulted in physio-chemical modifications of the original material, including an important increase in its specific surface area. The calcinated product proved to be suitable for the adsorption of RBB and Cr(VI) at low pH and temperature values.

Author Contributions: Conceptualization, I.B. and L.D.P.; methodology, I.B.; formal analysis, M.P.B.; investigation, I.B.; data curation, L.M. and M.C.; writing—original draft preparation, I.B., L.M. and M.P.B.; writing—review and editing, L.D.P. and V.P.; supervision, L.D.P. and V.P. All authors have read and agreed to the published version of the manuscript.

Funding: This research received no external funding.

Conflicts of Interest: The authors declare no conflict of interest.

References

1. Ahmad, R.; Mirza, A. Synthesis of Guar gum/bentonite a novel bionanocomposite: Isotherms, kinetics and thermodynamic studies for the removal of Pb (II) and crystal violet dye. *J. Mol. Liq.* **2018**, *249*, 805–814. [CrossRef]
2. Shirani, Z.; Santhosh, C.; Iqbal, J.; Bhatnagar, A. Waste Moringa oleifera seed pods as green sorbent for efficient removal of toxic aquatic pollutants. *J. Environ. Manag.* **2018**, *227*, 95–106. [CrossRef] [PubMed]
3. Natarajan, S.; Bajaj, H.C.; Tayade, R.J. Recent advances based on the synergetic effect of adsorption for removal of dyes from waste water using photocatalytic process. *J. Environ. Sci.* **2018**, *65*, 201–222. [CrossRef] [PubMed]
4. Taşar, Ş.; Kaya, F.; Özer, A. Biosorption of lead (II) ions from aqueous solution by peanut shells: Equilibrium, thermodynamic and kinetic studies. *J. Environ. Chem. Eng.* **2014**, *2*, 1018–1026. [CrossRef]

5. Wang, B.; Bai, Z.; Jiang, H.; Prinsen, P.; Luque, R.; Zhao, S.; Xuan, J. Selective heavy metal removal and water purification by microfluidically-generated chitosan microspheres: Characteristics, modeling and application. *J. Hazard. Mater.* **2019**, *364*, 192–205. [CrossRef] [PubMed]
6. Silva, B.; Neves, I.C.; Tavares, T. A sustained approach to environmental catalysis: Reutilization of chromium from wastewater. *Crit. Rev. Environ. Sci. Technol.* **2016**, *46*, 1622–1657. [CrossRef]
7. Rangabhashiyam, S.; Balasubramanian, P. Adsorption behaviors of hazardous methylene blue and hexavalent chromium on novel materials derived from Pterospermum acerifolium shells. *J. Mol. Liq.* **2018**, *254*, 433–445. [CrossRef]
8. Guo, H.; Bi, C.; Zeng, C.; Ma, W.; Yan, L.; Li, K.; Wei, K. Camellia oleifera seed shell carbon as an efficient renewable bio-adsorbent for the adsorption removal of hexavalent chromium and methylene blue from aqueous solution. *J. Mol. Liq.* **2018**, *249*, 629–636. [CrossRef]
9. Van Nguyen, N.; Lee, J.C.; Jeong, J.; Pandey, B.D. Enhancing the adsorption of chromium(VI) from the acidic chloride media using solvent impregnated resin (SIR). *Chem. Eng. J.* **2013**, *219*, 174–182. [CrossRef]
10. Dzakpasu, M.; Wu, K.; Chen, Z.; Yang, Q.; Liu, Z.; Yang, S.; Wang, W. Coagulation performance of cucurbituril for the removal of azo dyes: Effect of solution chemistry and coagulant dose. *Water Sci. Technol.* **2018**, *78*, 415–423. [CrossRef]
11. Petrucci, E.; Montanaro, D. Anodic oxidation of a simulated effluent containing Reactive Blue 19 on a boron-doped diamond electrode. *Chem. Eng. J.* **2011**, *174*, 612–618. [CrossRef]
12. Nidheesh, P.V.; Zhou, M.; Oturan, M.A. An overview on the removal of synthetic dyes from water by electrochemical advanced oxidation processes. *Chemosphere* **2018**, *197*, 210–227. [CrossRef]
13. Fu, F.; Wang, Q. Removal of heavy metal ions from wastewaters: A review. *J. Environ. Manag.* **2011**, *92*, 407–418. [CrossRef] [PubMed]
14. Di Palma, L.; Gueye, M.T.; Petrucci, E. Hexavalent chromium reduction in contaminated soil: A comparison between ferrous sulphate and nanoscale zero-valent iron. *J. Hazard. Mater.* **2015**, *281*, 70–76. [CrossRef] [PubMed]
15. Yagub, M.T.; Sen, T.K.; Afroze, S.; Ang, H.M. Dye and its removal from aqueous solution by adsorption: A review. *Adv. Colloid Interface Sci.* **2014**, *209*, 172–184. [CrossRef] [PubMed]
16. Ramesh, A.; Lee, D.J.; Wong, J.W.C. Thermodynamic parameters for adsorption equilibrium of heavy metals and dyes from wastewater with low-cost adsorbents. *J. Colloid Interface Sci.* **2005**, *291*, 588–592. [CrossRef]
17. Mohan, D.; Pittman, C.U. Activated carbons and low cost adsorbents for remediation of tri- and hexavalent chromium from water. *J. Hazard. Mater.* **2006**, *137*, 762–811. [CrossRef]
18. Ma, Y.; Liu, B.; Sun, N.; Ma, H.; Bao, L.; Cheng, H.; Zhou, J. Adsorption of Cr ions (VI) by modified activated carbon. *Chin. J. Environ. Eng.* **2014**, *8*, 2672–2676.
19. Chen, S.S.; Tung, K.L.; Abdolali, A.; Guo, W.S.; Ngo, H.H.; Nguyen, N.C. Typical lignocellulosic wastes and by-products for biosorption process in water and wastewater treatment: A critical review. *Bioresour. Technol.* **2013**, *160*, 57–66. [CrossRef]
20. Maletić, S.; Radonić, J.; Knudsen, T.S.; Igić, S.M.; Pap, S.; Turk Sekulić, M. Utilization of fruit processing industry waste as green activated carbon for the treatment of heavy metals and chlorophenols contaminated water. *J. Clean. Prod.* **2017**, *162*, 958–972. [CrossRef]
21. Rafatullah, M.; Sulaiman, O.; Hashim, R.; Ahmad, A. Adsorption of methylene blue on low-cost adsorbents: A review. *J. Hazard. Mater.* **2010**, *177*, 70–80. [CrossRef]
22. Ghorbel-Abid, I.; Galai, K.; Trabelsi-Ayadi, M. Retention of chromium (III) and cadmium (II) from aqueous solution by illitic clay as a low-cost adsorbent. *Desalination* **2010**, *256*, 190–195. [CrossRef]
23. Erdem, M.; Orhan, R.; Şahin, M.; Aydin, E. Preparation and Characterization of a Novel Activated Carbon from Vine Shoots by ZnCl2Activation and Investigation of Its Rifampicine Removal Capability. *Water Air Soil Pollut.* **2016**, *227*, 226. [CrossRef]
24. Ozdemir, I.; Şahin, M.; Orhan, R.; Erdem, M. Preparation and characterization of activated carbon from grape stalk by zinc chloride activation. *Fuel Process. Technol.* **2014**, *125*, 200–206. [CrossRef]
25. Agarski, B.; Radonic, J.; Vukelic, D.; Sekulic, M.T.; Budak, I.; Boskovic, N.; Pap, S. Eco-design of a low-cost adsorbent produced from waste cherry kernels. *J. Clean. Prod.* **2017**, *174*, 1620–1628. [CrossRef]
26. Farooq, U.; Kozinski, J.A.; Khan, M.A.; Athar, M. Biosorption of heavy metal ions using wheat based biosorbents—A review of the recent literature. *Bioresour. Technol.* **2010**, *101*, 5043–5053. [CrossRef] [PubMed]

27. Heck, C.I.; De Mejia, E.G. Yerba mate tea (Ilex paraguariensis): A comprehensive review on chemistry, health implications, and technological considerations. *J. Food Sci.* **2007**, *72*, R138–R151. [CrossRef]
28. Arreche, R.A.; de Oca-Vásquez, G.M.; Vega-Baudrit, J.R.; Vázquez, P.G. Synthesis of Silver Nanoparticles Using Extracts from Yerba Mate (Ilex paraguariensis) Wastes. *Waste Biomass Valorization* **2018**, 1–9. [CrossRef]
29. Vieira, M.A.; Maraschin, M.; Pagliosa, C.M.; Podestá, R.; de Simas, K.N.; Rockenbach, I.I.; Amboni, R.D.D.M.; Amante, E.R. Phenolic acids and methylxanthines composition and antioxidant properties of mate (ilex paraguariensis) residue. *J. Food Sci.* **2010**, *75*, C280–C285. [CrossRef]
30. Anesini, C.; López, P.; Ferraro, G.; Isolabella, S.; Cogoi, L.; Filip, R. Study of the bioactive compounds variation during yerba mate (Ilex paraguariensis) processing. *Food Chem.* **2010**, *122*, 695–699. [CrossRef]
31. Nunes, R.L.C.; Santacruz, G.; Arcaro, S.; Koop, A.A.; Pérez, B.C. Glass Foams Produced from Glass and Yerba Mate (Ilex paraguarinensis) Waste. *FME Trans.* **2018**, *46*, 70–79. [CrossRef]
32. Húmpola, P.; Odetti, H.; Moreno-Piraján, J.C.; Giraldo, L. Activated carbons obtained from agro-industrial waste: Textural analysis and adsorption environmental pollutants. *Adsorption* **2016**, *22*, 23–31. [CrossRef]
33. Albadarin, A.B.; Solomon, S.; Daher, M.A.; Walker, G. Efficient removal of anionic and cationic dyes from aqueous systems using spent Yerba Mate "Ilex paraguariensis". *J. Taiwan Inst. Chem. Eng.* **2018**, *82*, 144–155. [CrossRef]
34. Afolayan, O. The Efficacy of Banana Peel Activated Carbon in the Removal of Cyanide and Selected Metals from Cassava Processing Wastewater. *Adv. Res.* **2018**, 1–12. [CrossRef]
35. Bardestani, R.; Patience, G.S.; Kaliaguine, S. Experimental methods in chemical engineering: Specific surface area and pore size distribution measurements—BET, BJH, DFT. *Can. J. Chem. Eng.* **2019**, *97*, 2781–2791. [CrossRef]
36. Selambakkannu, S.; Othman, N.A.F.; Bakar, K.A.; Shukor, S.A.; Karim, Z.A. A kinetic and mechanistic study of adsorptive removal of metal ions by imidazole-functionalized polymer graft banana fiber. *Radiat. Phys. Chem.* **2018**, *153*, 58–69. [CrossRef]
37. United States Environmental Protection Agency (EPA). SW-846 Test Method 7196A: Chromium, Hexavalent (Colorimetric). Available online: http://www.epa.gov/hw-sw846/sw-846-test-method-7196a-chromium-hexavalent-colorimetric (accessed on 26 February 2019).
38. Bavasso, I.; Bracciale, M.P.; Sbardella, F.; Tirillò, J.; Sarasini, F.; Di Palma, L. Effect of yerba mate (Ilex paraguariensis) residue and coupling agent on the mechanical and thermal properties of polyolefin-based composites. *Polym. Compos.* **2020**, *41*, 161–173. [CrossRef]
39. Belhaine, A.; Ghezzar, M.R.; Abdelmalek, F.; Tayebi, K.; Ghomari, A.; Addou, A. Removal of methylene blue dye from water by a spent bleaching earth biosorbent. *Water Sci. Technol.* **2016**, 2534–2540. [CrossRef]
40. Nogueira, G.D.R.; Duarte, C.R.; Barrozo, M.A.S. Hydrothermal carbonization of acerola (Malphigia emarginata D. C.) wastes and its application as an adsorbent. *Waste Manag.* **2019**, *95*, 466–475. [CrossRef]
41. Gupta, V.K.; Jain, R.; Shrivastava, M.; Nayak, A. Equilibrium and Thermodynamic Studies on the Adsorption of the Dye Tartrazine onto Waste "Coconut Husks" Carbon and Activated Carbon. *J. Chem. Eng. Data* **2010**, *55*, 5083–5090. [CrossRef]
42. Glueckauf, E.; Coates, J.J. Theory of chromatography. Part IV. The influences of incomplete equilibrium on the front boundary of chromatograms and on the effectiveness of separation. *J. Chem. Soc.* **1947**, 1315–1321. [CrossRef] [PubMed]
43. Shi, J.; Yang, J.; Han, R.; Wang, Y.; Lu, Y.; Han, P. Removal of methylene blue from aqueous solution by chaff in batch mode. *J. Hazard. Mater.* **2006**, *137*, 550–557. [CrossRef]
44. Chen, J.; Yang, C.; Li, M.; Gong, R.; Sun, Y. Removal of cationic dyes from aqueous solution by adsorption on peanut hull. *J. Hazard. Mater.* **2005**, *121*, 247–250. [CrossRef]
45. Annadurai, G.; Juang, R.S.; Lee, D.J. Use of cellulose-based wastes for adsorption of dyes from aqueous solutions. *J. Hazard. Mater.* **2002**, *92*, 263–274. [CrossRef]
46. Vadivelan, V.; Kumar, K.V. Equilibrium, kinetics, mechanism, and process design for the sorption of methylene blue onto rice husk. *J. Colloid Interface Sci.* **2005**, *286*, 90–100. [CrossRef]
47. Sostaric, T.; Mineral, O.; Materials, R.; Milojkovic, J. Biosorption of methylene blue by waste apricot shells from food industry. *J. Eng. Process. Manag.* **2015**, *7*, 107–114. [CrossRef]
48. Bulut, Y.; Ayd, H. A kinetics and thermodynamics study of methylene blue adsorption on wheat shells. *Desalination* **2006**, *194*, 259–267. [CrossRef]

49. Franca, A.S.; Oliveira, L.S.; Ferreira, M.E. Kinetics and equilibrium studies of methylene blue adsorption by spent coffee grounds. *Desalination* **2009**, *249*, 267–272. [CrossRef]
50. Pavan, F.A.; Lima, E.C.; Dias, S.L.P.; Mazzocato, A.C. Methylene blue biosorption from aqueous solutions by yellow passion fruit waste. *J. Hazard. Mater.* **2008**, *150*, 703–712. [CrossRef]
51. Uddin, M.T.; Islam, M.A.; Mahmud, S.; Rukanuzzaman, M. Adsorptive removal of methylene blue by tea waste. *J. Hazard. Mater.* **2009**, *164*, 53–60. [CrossRef]
52. Annesini, M.C.; Marrelli, L.; Piemonte, V.; Turchetti, L. *Artificial Organ Engineering*; Springer: London, UK, 2017; ISBN 978-1-4471-6442-5. [CrossRef]
53. Leaist, D.G. The effects of aggregation, counterion binding, and added NaCl on diffusion of aqueous methylene blue. *Can. J. Chem.* **1988**, *66*, 2452–2457. [CrossRef]
54. Xie, Y.; Li, S.; Wang, F.; Liu, G. Removal of perchlorate from aqueous solution using protonated cross-linked chitosan. *Chem. Eng. J.* **2010**, *156*, 56–63. [CrossRef]
55. Gode, F.; Pehlivan, E. Removal of Cr(VI) from aqueous solution by two Lewatit-anion exchange resins. *J. Hazard. Mater.* **2005**, *119*, 175–182. [CrossRef] [PubMed]